Published in final edited form as:

Brain Struct Funct. 2015 September ; 220(5): 2639–2652. doi:10.1007/s00429-014-0815-8.

The superior paraolivary nucleus shapes temporal response properties of neurons in the inferior colliculus

Richard A. Felix II[1], **Anna K. Magnusson**[2], and **Albert S. Berrebi**[1]

[1]Department of Otolaryngology–Head and Neck Surgery and the Sensory Neuroscience Research Center, West Virginia University School of Medicine, Morgantown, West Virginia 26506 USA

[2]Center for Hearing and Communication Research, Karolinska Institutet and Department of Clinical Science, Intervention and Technology, Karolinska University Hospital, 17176 Stockholm, Sweden

Abstract

The mammalian superior paraolivary nucleus (SPON) is a major source of GABAergic inhibition to neurons in the inferior colliculus (IC), a well-studied midbrain nucleus that is the site of convergence and integration for the majority ascending auditory pathways en route to the cortex. Neurons in the SPON and IC exhibit highly precise responses to temporal sound features, which are important perceptual cues for naturally occurring sounds. To determine how inhibitory input from the SPON contributes to the encoding of temporal information in the IC, a reversible inactivation procedure was conducted to silence SPON neurons while recording responses to amplitude-modulated tones and silent gaps between tones in the IC. The results show that SPON-derived inhibition shapes responses of onset and sustained units in the IC via different mechanisms. Onset neurons appear to be driven primarily by excitatory inputs and their responses are shaped indirectly by SPON-derived inhibition, whereas sustained neurons are heavily influenced directly by transient offset inhibition from the SPON. The findings also demonstrate that a more complete dissection of temporal processing pathways is critical for understanding how biologically important sounds are encoded by the brain.

Keywords

amplitude modulation; gap detection; superior olive; sound envelopes; temporal processing

Introduction

The superior paraolivary nucleus (SPON) is a prominent GABAergic cell group located in the brainstem within the superior olivary complex, a group of auditory nuclei implicated in binaural sound localization (Saldaña and Berrebi 2000; Tollin 2003; Grothe et al. 2010). Unlike cells in neighboring nuclei, SPON neurons do not appear to play a major role in sound source localization (Behrend et al. 2002; Dehmel et al. 2002; Kulesza et al. 2003). A

Correspondence: Albert S. Berrebi, Sensory Neuroscience Research Center, PO Box 9303 HSC, Morgantown, WV 26506-9303, aberrebi@hsc.wvu.edu, ph: (304) 293-2357; fax: (304) 293-7182.

hallmark of the SPON neuronal response is well-timed transient spiking triggered by the offset of sound stimuli (Dehmel et al. 2002; Kulesza et al. 2003; Kadner et al. 2006; Kadner and Berrebi 2008). Because SPON-derived inhibition would manifest after sound stimulation ends, determining a clear role for the SPON in shaping response properties in target brain areas has been challenging.

Several hypotheses regarding potential roles of the SPON in ascending auditory pathways have been proposed including sound localization (Dehmel et al. 2002), rhythm coding (Felix et al. 2011) and gap detection (Kadner et al. 2006; Kopp-Scheinpflug et al. 2011), but the idea that has been explored most thoroughly is that the SPON functions as a discontinuity detector of temporal sound features (Kadner and Berrebi 2008). This view suggests that SPON neurons are specialized for signaling brief periods of low stimulus energy via offset inhibition. This characterization is based on observations that SPON neurons exhibit highly synchronous responses to changes in the amplitude of stimulus envelopes, and are able to detect very short gaps within ongoing sounds (Kuwada and Batra 1999; Behrend et al. 2002; Kulesza et al. 2003; Kadner and Berrebi 2008). Despite the fact that SPON neurons appear well-suited to encode stimulus discontinuities, how they impact auditory processing at the level of their primary target, the inferior colliculus (IC) remains unclear.

Properties of neurons in the central nucleus of the IC have been studied extensively with regard to responses to temporal sound features, including those of amplitude-modulated sounds (Langner 1992; Burger and Pollak 1998; Frisina 2001; Caspary et al. 2002; Zhang and Kelly 2003; Joris et al. 2004) and gap detection (Walton et al. 1997; Barsz et al. 1998; Wilson and Walton 2002; Allen et al. 2003). Because SPON neurons, like IC neurons, exhibit a high degree of sensitivity to similar ranges of sound envelope modulation frequencies and gaps in ongoing sounds (Walton et al. 1997; Yang and Pollak 1997; Krishna and Semple 2000; Zhang and Kelly 2006; Kadner and Berrebi 2008), it is reasonable to investigate how SPON inhibition modulates temporal responses of IC neurons.

To examine the degree to which SPON input mediates responses to temporal stimulus features in the IC, a reversible inactivation protocol was employed whereby SPON neurons were silenced via pharmacological blockade of neurotransmitter receptors. We targeted our recordings only to SPON-IC pairs of neurons with closely matched CFs, and responses of IC neurons to amplitude-modulated and gap stimuli were recorded before and during SPON inactivation.

Materials and methods

Surgical procedure

Twenty-five Sprague–Dawley rats (Harlan, Indianapolis, IN) weighing 175–250 grams were used for this study. All procedures conformed to the National Institutes of Health Guide for the Care and Use of Laboratory Animals and were approved by the West Virginia University Animal Care and Use Committee.

Deep surgical anesthesia was accomplished by injection of a mixture of ketamine (70 mg/kg) and xylazine (5 mg/kg) prior to surgery. The animal was then mounted in a

stereotaxic frame, a scalp incision was made, and connective tissue removed to expose the skull. A custom-made head post was secured to the skull with screws and dental cement. To gain access to the SPON, a craniotomy (3 × 7 mm) was opened with the rostral edge of the bone defect positioned near the caudal border of the transverse sinus. The dura mater was then removed and a portion of the exposed cerebellum aspirated to uncover the floor of the fourth ventricle, whose midline was used as a landmark for electrode penetrations. A second craniotomy (1 × 2 mm) was made for IC recordings approximately 0.5 mm lateral to the midline skull suture mark, with the caudal extent near the rostral border of the transverse sinus. The animal was then transferred to a sound-attenuated recording booth and placed on a thermostatically-controlled heating pad that maintained body temperature at 37°C and local anesthetic (5% lidocaine gel) was applied locally to the wound margins.

The depth of anesthesia was carefully monitored throughout the experiment by attending to physiological cues such as the rate and depth of respiration and the level of reflex activity. Supplemental doses of anesthetic (24 mg/kg ketamine) were given as needed to maintain adequate anesthesia at all times.

Sound delivery and recording procedure

Acoustic stimuli were created using custom software (BATLAB, Donald Gans, Northeast Ohio Medical University). Digital signals were converted to analog by a data acquisition processor (DAP5216a, Microstar Laboratories, Bellevue, WA) and passed through an anti-aliasing filter (FT6-2, Tucker-Davis Technologies (TDT), Alachua, FL). Sound level was controlled by programmable attenuators (PA-5, TDT) and signals were sent to speaker drivers (ED1, TDT) for presentation through free-field speakers (ES1, TDT) mounted to the stereotaxic frame approximately 5 mm from the opening of the ear canal. To avoid spectral contamination of stimuli by on and offset clicks, all stimuli were phased in and out using $\cos^2$ ramps (0.5 ms duration). The speaker output was calibrated ahead of the experiments using a condenser microphone (4939, Brüel and Kjaer North America, Norcross, GA) connected to a measuring amplifier (2610, Brüel and Kjaer). Based on this calibration, the speaker output was converted to dB SPL during data analysis. To ensure that monaural stimuli presented contralaterally were not stimulating the ipsilateral ear, acoustic crosstalk between the ears was estimated by presenting pure tones (0.5–60 kHz) from one speaker and comparing recordings of the tones obtained with a condenser microphone located in the position of each ear. The sound intensity measured at the position of the ear opposite the speaker location was consistently 35–40 dB lower than measurements from the ear closest to the speaker.

The SPON and central nucleus of the IC were located using stereotaxic coordinates from an atlas of the rat brain (Paxinos and Watson 1986). Single unit responses were recorded with glass pipette electrodes (tip diameters of 2–4 μm; 10–20 MΩ resistance) filled with 1.5% Biocytin (Sigma, St. Louis, MO) dissolved in 0.165M NaCl (pH 7.4). Electrode signals were amplified (2600, Dagan, Minneapolis, MN), bandpass filtered (200–3000 Hz; 3364 Krohn-Hite, Brockton, MA) and digitized at 42 kHz (DAP5216a, Microstar). Recordings from neurons were considered well isolated if the acoustically-evoked spike waveforms were homogeneous and could be reliably separated from background noise.

Procedure for inactivating the SPON

Prior to IC recordings, “piggyback” electrodes consisting of a single-barrel recording pipette glued onto a five-barrel drug delivery pipette were used for inactivation of SPON activity (Havey and Caspary 1980). Piggyback electrodes were constructed such that the tip of the recording pipette extended 20–30 μm beyond the tip of the multi-barrel pipette tip. The glycine receptor antagonist strychnine (10 mM; pH 3.0, Sigma) and the glutamate receptor antagonist kynurenic acid (100 mM; pH 8.5, Sigma), both dissolved in 0.165 M NaCl, were loaded into separate barrels. Drugs were delivered using iontophoresis (6400, Dagan) with ejection currents ranging from +10 to +40 nA for strychnine and −60 to −80 nA for kynurenic acid. Retention currents opposite the net charge of the drug solutions were applied during the search for neurons and during the baseline and recovery conditions of the recording protocol to prevent leakage of drug solutions from the pipette. One barrel of the piggyback electrode was filled with physiological saline and was used as a sum channel to balance the currents of the other drug barrels. Current was used to deliver vehicle solutions without drugs to ensure that the observed effects in the experiments were due to pharmacologic manipulation and not due to current application (Fig. 1A).

Electrodes were slowly advanced through the brainstem while a 50 ms broadband noise search stimulus was presented (~80 dB SPL, 4 presentations/s). SPON neurons were driven by contralateral stimulation and exhibited prominent spiking to the offset of the stimulus (Kulesza et al. 2003). Once a single-unit was isolated, its characteristic frequency (CF) and minimum threshold were determined audiovisually. The CF was defined as the frequency at which the lowest sound intensity was needed to evoke a response to at least half of the stimulus presentations and the threshold was the lowest sound intensity that elicited a response to half the stimulus presentations at the CF. Drugs were then delivered simultaneously from separate barrels of the pipette until the spiking rate of the unit decreased by at least 50%, which typically occurred within 10–15 minutes (Fig. 1B). After sufficient SPON inactivation, drug application was terminated and a washout period began until the neuron recovered spiking activity that approximated the baseline condition. The time courses for drug action and recovery were noted and the piggyback electrode was left in place while IC recordings were subsequently conducted using a second recording pipette (described below).

The distance between the recording and drug delivery pipettes was systematically varied in some experiments to estimate the extent and rate of drug diffusion within the SPON (Fig. 1C). Specifically, the separation of the recording and drug pipette tips was measured and correlated with the elapsed time from the start of the drug ejection and the inactivation of SPON activity, providing an approximation of the rate of drug spread (Burger and Pollak 2001). Due to the long time course of drug action involved in these experiments, no concurrent IC recordings were conducted.

Experimental paradigms

Following the confirmation of drug action and efficacy, the piggyback electrode was left in place in the SPON and a second recording electrode was advanced in the midbrain. Neurons in the central nucleus of the IC were distinguished from those in the neighboring dorsal

cortex of the IC by their characteristically higher thresholds and lower first spike latencies in response to pure tone stimuli (Palombi and Caspary 1996b; Lumani and Zhang 2010). We took advantage of the highly organized tonotopic projections from SPON to IC (Saldaña and Berrebi 2000; Saldaña et al. 2009) and recorded only those IC units whose CFs matched or were within 3 kHz of corresponding SPON units; this strategy maximized the likelihood that projections from targeted SPON neurons were functionally connected to units recorded in the IC.

Upon isolation of a single-unit in the IC, a peri-stimulus time histogram (PSTH) was recorded, first from the previously isolated SPON unit then immediately from the IC using the CF pure tones (100 presentations). Tones were 50 ms in duration and were presented at the IC unit's CF at 10 dB above the corresponding SPON unit's threshold. Following the recording of responses to pure tones, SAM tone and gap detection tests were also conducted for the IC unit in the *baseline* condition (described below). After the collection of baseline data, the recording protocols for pure tone, SAM and gap tests were repeated for the IC unit during the SPON *inactivation* condition. In some cases, data were collected from IC units in a *recovery* condition following the washout of drugs in the SPON.

Pure tone tests—To determine whether SPON offset spiking impacted the activity of IC neurons, a 10 ms analysis window was defined and the IC neuron's response rate was examined before and during SPON inactivation. The 10 ms offset analysis window was determined separately for each recorded pair of neurons and began at the time point of the shortest first-spike latency (FSL) of the SPON offset response (Fig. 2A). Spiking in this window was then measured for the IC unit's response in *baseline* and SPON *inactivation* conditions. To determine whether offset inhibition influenced the responses of units with no spontaneous activity, spiking was artificially elevated in some experiments by delivering a cocktail of glutamate and aspartate (500 mM, pH 8.0) iontophoretically via a second piggyback electrode positioned in the midbrain (Klug et al. 1999).

SAM tests—Stimuli consisted of 500 ms sinusoidally amplitude-modulated tones with the carrier frequency set at the IC unit's CF (100% modulation depth, 1 presentation/second) presented eight times per modulation frequency (MF). The time window for analyzing the entrainment of IC responses to cycles of amplitude modulation began 20 ms after the stimulus onset and ended at the offset (Fig. 2B). Responses to the first 20 ms of the stimulus were excluded from the analysis in order to minimize the influence of unsynchronized spikes associated with the stimulus onset on the calculation of the vector strength (see below). Spiking rates were determined and the synchronization of responses to each MF was quantified by calculating the vector strength (VS; Goldberg and Brown 1969) using the formula:

$$VS=\frac{1}{n}\sqrt{\left[\sum \sin(a_i)\right]^2+\left[\sum \cos(a_i)\right]^2}$$

where a_i is the phase angle of spike *I* relative to the modulation cycle of the stimulus, and *n* is the total number of spikes in the analysis window. To minimize the influence of isolated

spikes that were time-locked to the stimulus onset and thus occurred at a constant phase angle, the VS was set to 0 when the spike count fell to fewer than two spikes per stimulus presentation. A VS of 1 indicates perfect synchronization between the neuronal response and the modulation phase of the stimulus, whereas a VS of 0 indicates no correlation. The Rayleigh test (Batschelet 1981) was used to assess whether the distribution of spikes relative to the phase angle of the stimulus significantly differed from randomness. Period histograms were constructed for a subset of IC unit responses by plotting the phase angle of each spike relative to the amplitude modulation frequency of the stimulus.

Gap tests—A series of control tests were conducted to establish analysis windows for assessing gap detection (Fig. 2C; Kadner and Berrebi 2008). First, IC activity was recorded in a 300 ms recording window in the absence of sound stimulation to determine the spontaneous spiking rate for each neuron. Next, a 50 ms CF pure tone was presented (20 repetitions, 3 presentations/second) with a latency of 100 ms from the beginning of the recording window. This “leading marker” served as an indicator of the overall quality of the recording, as the response was presumed to remain consistent throughout the subsequent manipulation of stimuli. Next, responses to an identical “trailing marker” were recorded. The only difference between leading and trailing markers was their location within the recording window; the trailing marker latency was set at 150 ms, such that the leading and trailing markers abutted each other when presented in succession. The time period in the recording window corresponding to the first 10 ms of the trailing marker response was the analysis window used for all gap tests. The final control test replaced the 50 ms leading and trailing markers with a continuous 100 ms tone. Spiking in the analysis window for this test served as a control by which gap detection could be measured. Following these control tests, the leading and trailing markers were presented in succession as the gap durations between the two were systematically varied from 0 to 10 ms in increments of 1 ms. The 0 ms gap condition was constructed such that the end of the 0.5 ms offset ramp of the leading marker occurred at the same time as the start of the 0.5 ms onset ramp of the trailing marker. Thus, there was no true silent period between markers in the 0 ms gap condition, but a brief epoch of decreased energy was present compared to the period in the continuous tone condition. Gap detection by IC neurons before and during SPON inactivation was determined by the minimum gap threshold (MGT), defined as the shortest gap between leading and trailing markers that evoked distinct spiking responses to each tone. Responses were considered to be evoked by the trailing marker when the spiking rate in the analysis window changed by at least 50% compared to the same period in the continuous tone condition.

Histological localization of recording sites

Following the completion of the recording protocol, biocytin tracer deposits were made at the recording site in each nucleus to confirm that neurons were all located within the borders of the SPON or central nucleus of the IC (Fig. 3). This was done by applying anodic current of 1–2 μA through the electrode for 5–10 min (50% duty cycle; Fig. 3). Histological procedures were then conducted to reveal the deposits, as described previously (Kadner and Berrebi 2008). Briefly, after each experiment, and while still under deep surgical anesthesia, animals were perfused through the ascending aorta with physiological saline followed by 4% paraformaldehyde in 0.12 M sodium phosphate buffer (pH 7.2). The brain was then

removed from the cranium, cryoprotected overnight with 30% sucrose in 0.12 M sodium phosphate buffer and sectioned in the coronal plane (40 μm) on a freezing microtome. Free-floating sections were processed according to the ABC method (Vector Laboratories, Burlingame, CA) using diaminobenzidine as the chromogen.

Results

A total of 24 pairs of neurons were recorded from the SPON and IC with characteristic frequencies (CFs) between 5 and 33 kHz, covering the most sensitive range of hearing in the rat (Kelly and Masterton 1977). For each set of recordings, responses of IC neurons to pure tone, SAM and gap stimuli were conducted before and during SPON inactivation. To assess the effects of SPON input on differing cell types, IC responses were classified as either *onset* cells, which responded with brief spiking triggered by the stimulus onset, or *sustained* cells which exhibited spiking throughout the stimulus presentation.

IC responses to pure-tone stimuli

To test whether the SPON contributed to pure tone responses in the IC, spiking was measured in a brief time window following the stimulus offset for IC recordings before and during SPON inactivation (Fig. 4, shaded areas). The time window corresponded to the period when SPON neurons produced action potentials, as measured with a separate electrode in the SPON immediately prior to each IC recording. The spiking rate for onset IC units (n = 10) in the offset analysis window in the baseline condition (5.75 ± 0.2 spikes/s) did not change following inactivation of the SPON (6.13 ± 0.1 spikes/s; Wilcoxon signed-rank test, $p > 0.9$). Onset units were marked by little or no spontaneous and evoked activity for both baseline and SPON inactivation conditions, making it difficult to resolve the presence of SPON inputs (Fig. 4A). Thus, to better detect the presence of SPON-derived inhibition, the overall spiking rate was artificially elevated throughout the recording window (Burger and Pollak 2001) for a subset of IC recordings (n = 3) by applying a combination of glutamate and aspartate (Fig. 4B). By inducing a general increase in IC unit activity, we predicted that the SPON's inhibitory input would be apparent as a period of suppressed spiking in the background activity. Overall, spiking activity in the analysis window when the SPON input was intact did not differ (38.6 ± 10.7 spikes/s) when compared to a 10 ms control window that preceded the stimulus presentation prior to sound stimulation (40.01 ± 9.6 spikes/s), leaving the presence of functional SPON inputs unresolved. To further examine this question, spiking in the analysis window before and after SPON inactivation was measured in the presence of glutamate and aspartate (Fig. 4B, C). Although the average spiking rate in the analysis window in the baseline condition (38.6 ± 10.7 spikes/s) increased during SPON inactivation (49.3 ± 18.2 spikes/s), the variability was high and the sample size (n = 3) was too small to permit a statistical comparison. Sustained IC units (n = 10) typically had evoked spiking that persisted beyond the termination of the pure tone stimulus, thus glutamate and aspartate were not used to elevate the background activity for these units. Following SPON inactivation a higher average spiking rate was observed in the analysis window (39.45 ± 8.6 spikes/s) compared to the baseline condition (29.45 ± 5.9 spikes/s) (Fig. 4D, E), although the difference did not reach statistical significance (Wilcoxon signed-rank test, $p = 0.5$; Fig. 4F).

IC responses to SAM stimuli

The onset IC unit shown in Figure 5A responded best to a SAM tone with a 40 Hz MF in the baseline condition (top left panel). Spiking for this unit was entrained to a very limited range of MFs (40–80 Hz) over which significant vector strengths were calculated (VS = 0.76 to 0.83; Rayleigh test, p = 0.01 to 0.05). When the SPON was inactivated, both the spiking rate and vector strength dropped, resulting in a loss of phase-locking (Fig. 5A middle left panel). After the inactivating drugs were allowed to wash out, a partial recovery was observed, although the spiking rate and vector strength remained depressed compared to baseline (Fig. 5A bottom left panel). Although SPON inactivation altered the phase-locking ability of this unit compared to baseline, there was no apparent difference in the corresponding phase plots that were constructed for each condition (Fig. 5A right panels). Specifically, spiking was evoked primarily by one-third of each modulation cycle in the baseline, SPON inactivation and recovery conditions. Overall, vector strengths for the onset unit were substantially reduced during SPON inactivation for the range of MFs at which the unit phase-locked to in the baseline condition (40–80 Hz; Fig. 5C). Moreover, a partial recovery was observed after an hour of drug wash out at 40–80 Hz MF, but the statistically significant phase-locking observed in the baseline condition was not reached (Fig. 5C; Rayleigh test, p= 0.09 to 0.21 for tests conducted for each MF).

The sustained IC unit shown in Figure 5B also exhibited significant phase-locking to low MFs and spiking that was evoked by a specific portion of the modulation phase under baseline conditions (top panels). Compared to the onset unit, the sustained neuron responded to higher MFs, although these responses were not robust. During SPON inactivation, the response magnitude to the best MF of 40 Hz showed little change; however, phase-locking was lost (Rayleigh test, p = 0.31; Fig. 5B middle left panel). In contrast to the onset unit, the loss of spiking precision for the sustained unit was also evident in the corresponding phase plots, where a loss of selectivity to the modulation phase was clearly seen during SPON inactivation (Fig. 5B middle right panel). Although the degree of entrainment to the SAM tone was nearly significant following a recovery from SPON inactivation (Rayleigh test, p = 0.06), the response did not reach the degree of synchrony to the modulation cycles that was present in the baseline condition. Overall, SPON inactivation impaired entrainment of the sustained response to the SAM stimulus at 20 and 40 Hz MF in particular, although a clear recovery was not observed even one hour after the cessation of iontophoresis (Fig. 5D).

For this sample of onset (n = 8) and sustained (n = 6) IC neurons, all had bandpass modulation transfer functions in which spiking was not entrained to the lowest MF presented, nor to MFs above 180 Hz (Fig. 6). As a group, onset cells had significant phase-locking (Rayleigh test, p = 0.001 to 0.01) in response to 40, 60 and 80 Hz MFs in the baseline condition, with vector strengths averaging 0.78 ± 0.04, 0.73 ± 0.07 and 0.70 ± 0.07, respectively (Fig. 6A). During SPON inactivation, vector strengths for this range of MFs dropped to 0.49 ± 0.13, 0.50 ± 0.13, 0.41 ± 0.12, resulting in a loss of phase-locking (Rayleigh test, p = 0.14 to 0.26). In addition, the drops in baseline vector strengths at 40–80 Hz MF following inactivation were statistically significant (Wilcoxon signed-rank test, $p < 0.05$). Although SPON inactivation resulted in changes to vector strengths observed for onset units, no statistically significant change in spiking was observed across the MFs tested

(Wilcoxon signed-rank test, $p > 0.05$) despite lower average spiking rates for 40–100 Hz MF (Fig. 6B). For sustained IC units, average vector strengths were lower in response to 80–120 Hz MF, but these differences did not reach statistical significance for our population of neurons (Wilcoxon signed-rank test, $p = 0.16$ to 0.93; Fig. 6C). Furthermore, average spiking rates were lower at 100–180 Hz MF during SPON inactivation, but these changes were not significant (Fig. 6D).

IC responses to gap stimuli

A gap detection paradigm was employed whereby two identical CF tones were presented with a silent gap between that was systematically varied from 0 to 10 ms in 1 ms steps. Additional gaps of 15 and 20 ms were presented to confirm that there was no difference in spiking compared to the 10 ms gap response (Wilcoxon signed-rank test, $p > 0.05$ for all conditions). Thus, a plateau in gap-evoked spiking rates occurred by the 10 ms gap condition and did not increase further. Prior to manipulating the gap duration, a series of control tests were conducted beginning with the measurement of spontaneous activity by recording with no sound stimulation (N condition; Fig. 7 top panels). Typically, onset IC units had very little spontaneous activity (7.8 ± 2.6 spikes per second; Fig. 7A), while sustained units had much higher levels of spiking in the no sound condition (169.7 ± 27.9 spikes per second; Fig. 7B). The next set of control tests measured responses to the leading and trailing tone markers presented in isolation (L and T conditions, respectively; Fig. 7A, B). The first 10 ms of the response to the trailing marker (Fig. 7, shaded area) was used in all tests to assess gap detection by using this time window to compare spiking to various gap durations. The reference point for gap tests was the spiking rate in the analysis window of the continuous tone (C) control condition.

An example of an onset IC unit is shown in Figure 7A. This neuron had a minimum gap threshold (MGT), the minimum gap duration that elicited a response, of 5 ms. For the baseline condition, the response magnitude for this unit increased systematically from 0.2 spikes per stimulus at 5 ms gap to 0.5 spikes at 10 ms gap duration. During SPON inactivation, the MGT increased to 8 ms and only reached 0.4 spikes per stimulus at 10 ms gap duration. For both baseline and SPON inactivation conditions, gap evoked spiking was depressed compared to the response to the trailing marker alone, even for longest gaps presented (Fig. 7A). The sustained unit shown in Figure 7B had a clear response to the trailing marker (1.2 spikes per stimulus) when the gap duration was 0 ms. Spiking to the trailing marker was presumably evoked by the brief period of decreased energy introduced by the stimulus on/off ramps (see Methods). The response magnitude for the sustained unit increased with increasing gap duration in the baseline condition to reach 1.9 spikes per stimulus for the 10 ms gap. During SPON inactivation, the MGT increased to 4 ms and spiking increased from 0.5 spikes per stimulus at 4 ms gap duration to 0.9 spikes per stimulus at 8 ms duration, the point at which the response saturated. Although the spiking magnitude in the analysis window decreased during SPON inactivation for all gap durations, it must be noted that overall, spiking in the entire recording window decreased during SPON inactivation for all conditions (Fig. 7B bottom panels).

Responses to gaps of 0 to 10 ms are shown for populations of onset (n = 6) and sustained IC units (n = 6) before and during SPON inactivation (Fig. 8). For both response types, there were no significant differences in spiking in control tests before and during SPON inactivation (N, L, T, C conditions, Fig. 8A, B). For the population of onset IC units, there was a significant increase in spiking with increasing gap duration for both the baseline (Spearman's rank correlation, $r = 0.91$, $p < 0.001$) and SPON inactivation ($r = 0.90$, $p < 0.001$) conditions. However, for all gap durations (0–10 ms), there was no significant difference in spiking rate when baseline and SPON inactivation conditions were compared to each other (Friedman test, $p = 0.89$; Fig. 8A). In contrast to onset unit responses, the magnitude of gap evoked spiking did not depend on gap duration for sustained units (n = 6; Spearman's rank correlation, $r = -0.13$, $p = 0.71$). Specifically, sustained unit spiking was robust even in response to the shortest gaps. During SPON inactivation, spiking to very short gaps was reduced significantly, resulting in a monotonic relationship between spiking rate and gap duration, similar to the behavior seen in onset cells (Spearman's rank correlation, $r = 0.96$, $p < 0.001$; Fig. 8B). In addition, spiking rates were significantly lower for the SPON inactivation condition (Friedman test, $p = 0.03$) to all gaps shorter than 4 ms (Wilcoxon signed-rank test, $p < 0.05$) compared to baseline (Fig. 8B). Overall, there was no significant difference in MGTs for the SPON inactivation condition (5.5 ± 2.1 ms) compared to baseline (4.3 ± 1.2 ms) for onset units (Wilcoxon signed-rank test, $p = 0.13$; Fig. 8C). In contrast, baseline gap detection thresholds for sustained units (2.4 ± 0.9 ms) were significantly elevated when the SPON was inactivated (5.6 ± 1.0 ms; Wilcoxon signed-rank test, $p = 0.03$; Fig. 8C).

Discussion

This study demonstrates that synaptic input from the superior paraolivary nucleus (SPON)6 influences response properties of neurons in its primary target, the central nucleus of the inferior colliculus (IC). Both the SPON and IC are important centers for processing auditory cues in the temporal domain (Frisina 2001; Joris et al. 2004; Kadner and Berrebi 2008; Zheng and Escabi 2008; Felix et al. 2011; Kopp-Scheinpflug et al. 2011), but how the response properties of different subclasses of IC neurons relate to their plethora of synaptic inputs, some of which originate from SPON, has been difficult to establish. In particular, the precise role of inhibition in shaping the coding of temporal and spectral sound attributes in the IC has been the focus of intense study. Based on pharmacological blockade of postsynaptic inhibitory receptors in the IC (Burger and Pollack 1998; Caspary et al. 2002; Zhang and Kelly 2003), it has been reasoned that inhibition gates overall spiking selectivity, in essence creating a gain control mechanism (Gittelman at el. 2012). The present results demonstrate that selective inactivation of SPON-derived inhibition to the IC neurons reduces entrainment of their responses to SAM stimuli and increases their gap detection thresholds, without significantly changing their spiking activity. The data imply that precisely-timed inhibition from the SPON can drive individual IC neurons through differential mechanisms, depending on the neuron's integrative properties.

Inactivation of SPON neurons

Virtually all SPON neurons target the central nucleus of the IC and these connections are strictly topographic (Saldaña and Berrebi 2000; Saldaña et al. 2009). Thus, recordings were obtained from SPON-IC neuron pairs with closely matched CFs. Prior to recording in the IC, antagonists applied in the SPON were given enough time to silence projections to the individual IC unit under investigation (see Methods, Fig. 1C). However, the length of the protocol was also limited to avoid the spread of blockers into neighboring auditory nuclei, namely the lateral (LSO) and medial superior (MSO) olives and the medial nucleus of the trapezoid body (MNTB), that influence the IC either directly or indirectly (Faye-Lund 1986; Coleman and Clerici 1987; Kelly et al. 1998). Even if the duration of the recording protocol resulted in the spread of blockers outside the borders of the SPON, the known tonotopic organization of superior olivary nuclei indicates that affected neurons in these neighboring nuclei would have a negligible impact on our IC recordings, as their CFs would not match those of the SPON-IC unit pair under investigation. Specifically, low CF SPON neurons are located laterally within the nucleus, closest to high CF cells found in the medial-most region of the LSO; likewise, high-CF units are situated in the medial SPON, closest in proximity to the lowest CF cells found in the lateral portion of MNTB. Therefore, it is unlikely that excessive drug spread caused unspecific effects during the SPON inactivation procedure.

Effects of SPON inactivation on IC pure tone responses

Removing SPON-derived inhibition was expected to increase spiking in the IC, similar to studies in which large increases in spiking activity were observed in the IC when inhibition was antagonized locally (Burger and Pollak 1998; Caspary et al. 2002; Zhang and Kelly 2003). However, the modest changes in spiking activity observed during SPON inactivation did not reach statistical significance. Because significant effects were elicited in response to SAM and gap stimuli after inactivation, we surmise that pure tone stimuli are not optimal cues for elucidating the functional role of the SPON-to-IC circuit. The IC is the first site in the auditory system where virtually all lower ascending processing pathways converge (Winer and Schreiner 2005). Moreover, the IC consists of an intricate network of intrinsic and commissural connections (Saldaña and Merchan 2005). As a result of this integration of inputs, there is an emergence of neuronal selectivity to increasingly complex stimuli compared to cells in lower brainstem nuclei (Bauer et al. 2002; Portfors and Felix 2005; Pollak et al. 2011; Pollak 2013). Therefore, it is reasonable that the effect of inactivating SPON inputs would be more pronounced when sounds contained stimulus features for which both IC and SPON neurons are uniquely tuned, such as low-rate envelope amplitude modulations or short gaps in ongoing stimuli (Walton et al. 1997; Krishna and Semple 2000; Kadner and Berrebi 2008).

SPON inactivation altered IC responses to SAM tones

For onset units in the central nucleus of the IC, silencing SPON-derived inhibition caused a reduction in vector strengths over the range of MFs for which SPON and IC neurons are most sensitive (Krishna and Semple 2000; Kulesza et al. 2003). Thus, it is tempting to speculate that selective synchronization to lower MFs is a result of the manner in which the arrival of excitatory and inhibitory inputs overlap for onset neurons. Conceptual models

have been constructed in which delayed inhibition allows unmasked excitatory input to drive SAM responses until the MF reaches a point where the arrival of the excitation and inhibition overlap and cancel each other, resulting in a loss of phase-locking (Grothe 1994; Yang and Pollak 1997). However, the results herein imply that the network may be more complex, since firing rates decreased somewhat for the selective MFs and in some cases exhibited subtle increases for the unselective MFs. Such effects may be achieved if inhibitory interneurons are considered in the network (Oliver and Morest 1984; Malmierca et al. 2009). For example, a timed disinhibition mediated by the SPON would enhance the IC SAM response up to the MF limit of SPON neurons (Kuwada and Batra 1999; Kadner and Berrebi 2008; Felix et al. 2012). In this scenario, abolishing the SPON input would unmask a potentially tonic inhibition from interneurons, which would smear the synchronization of the response without substantially affecting the overall spiking activity. In line with our findings, Burger and Pollak (1998) reported decreased vector strengths in response to low MF SAM tones when postsynaptic inhibition mediated by the $GABA_A$ receptor was antagonized pharmacologically in the IC. In the same study, the range of MFs to which IC units phase locked did not change, which is also in agreement with our findings.

Previous studies that blocked $GABA_A$ receptors locally in the IC reported that the overall spiking rate of neurons increased substantially at virtually all MFs tested (Burger and Pollak 1998; Zhang and Kelly 2003); whereas our results showed no significant change in spiking, even at MFs for which vector strengths were substantially affected by SPON inactivation. Hence, the reduction in phase-locking for onset cells that we observed is not due to changes in spiking activity. In contrast, a non-specific blockade of GABAergic inputs to IC neurons (including those originating from the SPON, nuclei of the lateral lemniscus and contralateral IC, as well as local interneurons) has pronounced widespread effects on overall neuronal excitability to a variety of stimuli for all cell types tested (Palombi and Caspary 1996a; Burger and Pollak 1998; Zhang and Kelly 2003).

SPON inactivation increased gap detection thresholds for sustained IC units

Sustained IC neurons had significant increases in gap detection thresholds during SPON inactivation and onset units displayed a similar trend, but differences were not statistically significant. Moreover, spiking rates during inactivation decreased for sustained IC units to all gap durations, particularly for very short gaps (< 4 ms). One potential explanation for these observations involves so-called rebound spiking following release from SPON-derived inhibition. Rebound spiking, caused by the hyperpolarization-activated h and calcium currents, has been shown to underlie offset spiking responses to tones in the SPON *in vivo* (Felix et al. 2011) and has also been described in the rat and gerbil IC (Sivaramakrishnan and Oliver 2001; Koch and Grothe 2003; Sun and Wu 2008). The fact that spiking triggered by the shortest sound gaps in sustained units was abolished by SPON inactivation strongly suggests that this response is driven by inhibition. This is in stark contrast to the gap detection thresholds of onset cells, which were virtually unaffected by inactivation. The clear association between IC response types and mechanisms of gap detection suggests that onset cells are primarily driven by an excitatory input; in the gap detection paradigm, onset cells would consequently respond to the onset of the trailing marker whenever the gap

duration is long enough to overcome the refractory period of the leading marker response and inhibitory network effects.

Another important consequence of a rebound spiking mechanism in sustained IC neurons is their high sensitivity to SAM stimuli shown in this study. Rebound spiking, triggered at the upstroke of the signal, acting in tandem with an excitatory input, could extend the coding range of modulation frequencies in both directions. On the one hand, a more sluggish inhibitory rebound may boost the response to low MFs, as with gap detection; on the other hand, the hyperpolarization-activated currents may decrease the electrical time constants and act as a high-pass filter (Cangiano et al. 2007) of sustained neurons and thereby make them more responsive to higher MFs. This is one possible explanation for our finding that changes in vector strengths and spiking of sustained units were manifest primarily at higher MFs during SPON inactivation (Fig. 6C, D). We speculate that sustained neurons are preserving coarse temporal information through a rebound mechanism with high precision, thus making them suitable sound gap detectors.

Potential roles for the SPON in processing temporal sound cues

The findings presented herein support the notion that the SPON contributes to the creation of selectivity for temporal cues at the level of the IC. Interestingly, the well-timed inhibition from the SPON appears to affect two classes of IC neurons via vastly different mechanisms – in the case of sustained neurons, the effects seemed to be mediated through neuronal integration of inhibitory inputs, and in the case of onset cells, through neuronal integration of excitatory inputs; both mechanisms would rely on specific intrinsic cellular and local network properties. This could explain why previous studies presented a mixed picture of the degree to which inputs from subcollicular nuclei contribute to IC responses to complex acoustic stimuli (Koch and Grothe 1998; Burger and Pollak 2001; Caspary et al. 2002; Zhang and Kelly 2003). Our results also invite a more detailed dissection of the neural circuitry of the IC, including examination of a recently described periodicity map organized perpendicular to the established tonotopic map (Baumann et al. 2010).

We propose that the SPON is a critical component of pathways that convey the coarse temporal structure of sounds by providing well-timed inhibition that enables IC neurons to segment cycles of amplitude modulation with greater fidelity, and to detect short gaps within ongoing sounds. The temporal code preserved in sound energy fluctuations is essential for speech perception (Drullman 1995; Shannon et al. 1995), auditory streaming (Shamma and Micheyl 2010) and increasing the signal-to-noise ratio in noisy environments (Zwicker 1985; Henry and Heinz 2012; Anderson et al. 2013). Therefore, mapping out the neural pathways and circuits that carry acoustic timing information and understanding their underlying mechanisms will be of great importance for our understanding of communication in a variety of mammalian species.

Acknowledgments

This work was supported by NIH/National Institute on Deafness and Other Communication Disorders Grant RO1 DC-002266 (A.S.B). R.A.F. II was supported, in part, by training grant T32 GM081741 from the NIH/National Institute of General Medical Sciences to West Virginia University.

References

Allen PD, Burkard RF, Ison JR, Walton JP. Impaired gap encoding in aged mouse inferior colliculus at moderate but not high stimulus levels. Hear Res. 2003; 186:17–29. [PubMed: 14644456]

Anderson S, Parbery-Clark A, White-Schwoch T, Drehobl S, Kraus N. Effects of hearing loss on the subcortical representation of speech cues. J Acoust Soc Am. 2013; 133:3030–3038. [PubMed: 23654406]

Barsz K, Ison JR, Snell KB, Walton JP. Behavioral and neural measures of auditory temporal acuity in aging humans and mice. Neurobiol Aging. 2002; 23:565–578. [PubMed: 12009506]

Batschelet, E. Circular statistics in biology. Academic Press; London: 1981.

Bauer EE, Klug A, Pollak GD. Features of contralaterally evoked inhibition in the inferior colliculus. Hear Res. 2000; 141:80–96. [PubMed: 10713497]

Baumann S, Griffiths TD, Rees A, Hunter D, Sun L, Thiele A. Characterization of the BOLD response time course at different levels of the auditory pathway in non-human primates. Neuroimage. 2010; 50:1099–1108. [PubMed: 20053384]

Behrend O, Brand A, Kapfer C, Grothe B. Auditory response properties in the superior paraolivary nucleus of the gerbil. J Neurophysiol. 2002; 87:2915–2928. [PubMed: 12037195]

Burger RM, Pollak GD. Analysis of the role of inhibition in shaping responses to sinusoidally amplitude-modulated signals in the inferior colliculus. J Neurophysiol. 1998; 80:1686–1701. [PubMed: 9772232]

Burger RM, Pollak GD. Reversible inactivation of the dorsal nucleus of the lateral lemniscus reveals its role in the processing of multiple sound sources in the inferior colliculus of bats. J Neurosci. 2001; 21:4830–4843. [PubMed: 11425910]

Cangiano L, Gargini C, Della Santina L, Demontis GC, Cervetto L. High-pass filtering of input signals by the I_h current in a non-spiking neuron, the retinal rod bipolar cell. PLoS One. 2007; 2:e1327. [PubMed: 18091997]

Caspary DM, Palombi PS, Hughes LF. GABAergic inputs shape responses to amplitude modulated stimuli in the inferior colliculus. Hear Res. 2002; 168:163–173. [PubMed: 12117518]

Coleman JR, Clerici WJ. Sources of projections to subdivisions of the inferior colliculus in the rat. J Comp Neurol. 1987; 262:215–226. [PubMed: 3624552]

Dehmel S, Kopp-Scheinpflug C, Dorrscheidt GJ, Rubsamen R. Electrophysiological characterization of the superior paraolivary nucleus in the Mongolian gerbil. Hear Res. 2002; 172:18–36. [PubMed: 12361864]

Drullman R. Temporal envelope and fine structure cues for speech intelligibility. J Acoust Soc Am. 1995; 97:585–592. [PubMed: 7860835]

Faingold CL, Travis MA, Gehlbach G, Hoffmann WE, Jobe PC, Laird HE, Caspary DM. Neuronal response abnormalities in the inferior colliculus of the genetically epilepsy-prone rat. Electroencephalogr Clin Neurophysiol. 1986; 63:296–305. [PubMed: 2419087]

Faye-Lund H. Projection from the inferior colliculus to the superior olivary complex in the albino rat. Anat Embryol (Berl). 1986; 175:35–52. [PubMed: 3026205]

Felix RA, Fridberger A, Leijon S, Berrebi AS, Magnusson AK. Sound rhythms are encoded by post-inhibitory rebound spiking in the superior paraolivary nucleus. J Neurosci. 2011; 31:12566–12578. [PubMed: 21880918]

Felix RA, Kadner A, Berrebi AS. Effects of ketamine on response properties of neurons in the superior paraolivary nucleus of the mouse. Neuroscience. 2012; 201:307–319. [PubMed: 22123167]

Frisina RD. Subcortical neural coding mechanisms for auditory temporal processing. Hear Res. 2001; 158:1–27. [PubMed: 11506933]

Gittelman JX, Wang L, Colburn HS, Pollak GD. Inhibition shapes response selectivity in the inferior colliculus by gain modulation. Front Neural Circuits. 2012; 18;6:67.

Goldberg JM, Brown PB. Response of binaural neurons of dog superior olivary complex to dichotic tonal stimuli: some physiological mechanisms of sound localization. J Neurophysiol. 1969; 32:613–636. [PubMed: 5810617]

Grothe B. Interaction of excitation and inhibition in processing of pure tone and amplitude-modulated stimuli in the medial superior olive of the mustached bat. J Neurophysiol. 1994; 71:706–721. [PubMed: 8176433]

Grothe B, Pecka M, McAlpine D. Mechanisms of sound localization in mammals. Physiol Rev. 2010; 90:983–1012. [PubMed: 20664077]

Havey DC, Caspary DM. A simple technique for constructing “piggyback” multibarrel microelectrodes. Electroencephalogr Clin Neurophysiol. 1980; 48:249–251. [PubMed: 6153344]

Henry KS, Heinz MG. Diminished temporal coding with sensorineural hearing loss emerges in background noise. Nat Neurosci. 2012; 15:1362–1364. [PubMed: 22960931]

Joris PX, Schreiner CE, Rees A. Neural processing of amplitude-modulated sounds. Physiol Rev. 2004; 84:541–577. [PubMed: 15044682]

Kadner A, Berrebi AS. Encoding of temporal features of auditory stimuli in the medial nucleus of the trapezoid body and superior paraolivary nucleus of the rat. Neuroscience. 2008; 151:868–887. [PubMed: 18155850]

Kadner A, Kulesza RJ, Berrebi AS. Neurons in the medial nucleus of the trapezoid body and superior paraolivary nucleus of the rat may play a role in sound duration coding. J Neurophysiol. 2006; 95:1499–1508. [PubMed: 16319207]

Kelly JB, Liscum A, del van AB, Ito M. Projections from the superior olive and lateral lemniscus to tonotopic regions of the rat’s inferior colliculus. Hear Res. 1998; 116:43–54. [PubMed: 9508027]

Kelly JB, Masterton B. Auditory sensitivity of the albino rat. J Comp Physiol Psychol. 1977; 91:930–936. [PubMed: 893752]

Klug A, Bauer EE, Pollak GD. Multiple components of ipsilaterally evoked inhibition in the inferior colliculus. J Neurophysiol. 1999; 82:593–610. [PubMed: 10444659]

Koch, Grothe. GABAergic and glycinergic inhibition sharpens tuning for frequency modulations in the inferior colliculus of the big brown bat. J Neurophysiol. 1998; 80:71–82. [PubMed: 9658029]

Koch U, Grothe B. Hyperpolarization-activated current (Ih) in the inferior colliculus: distribution and contribution to temporal processing. J Neurophysiol. 2003; 90:3679–3687. [PubMed: 12968010]

Kopp-Scheinpflug C, Tozer AJ, Robinson SW, Tempel BL, Hennig MH, Forsythe ID. The sound of silence: ionic mechanisms encoding sound termination. Neuron. 2011; 71:911–925. [PubMed: 21903083]

Krishna BS, Semple MN. Auditory temporal processing: responses to sinusoidally amplitude-modulated tones in the inferior colliculus. J Neurophysiol. 2000; 84:255–273. [PubMed: 10899201]

Kulesza RJ, Berrebi AS. Superior paraolivary nucleus of the rat is a GABAergic nucleus. J Assoc Res Otolaryngol. 2000; 1:255–269. [PubMed: 11547806]

Kulesza RJ, Kadner A, Berrebi AS. Distinct roles for glycine and GABA in shaping the response properties of neurons in the superior paraolivary nucleus of the rat. J Neurophysiol. 2007; 97:1610–1620. [PubMed: 17122321]

Kulesza RJ, Spirou GA, Berrebi AS. Physiological response properties of neurons in the superior paraolivary nucleus of the rat. J Neurophysiol. 2003; 89:2299–2312. [PubMed: 12612016]

Kuwada S, Batra R. Coding of sound envelopes by inhibitory rebound in neurons of the superior olivary complex in the unanesthetized rabbit. J Neurosci. 1999; 19:2273–2287. [PubMed: 10066278]

Langner G. Periodicity coding in the auditory system. Hear Res. 1992; 60:115–142. [PubMed: 1639723]

Lumani A, Zhang H. Responses of neurons in the rat’s dorsal cortex of the inferior colliculus to monaural tone bursts. Brain Res. 2010; 1351:115–129. [PubMed: 20615398]

Malmierca MS, Hernandez O, Antunes FM, Rees A. Divergent and point-to-point connections in the commissural pathway between the inferior colliculi. J Comp Neurol. 2009; 514:226–239. [PubMed: 19296464]

Oliver DL, Morest DK. The central nucleus of the inferior colliculus of the cat. J Comp Neurol. 222:237–264. [PubMed: 6699209]

Palombi PS, Caspary DM. GABA inputs control discharge rate primarily within frequency receptive fields of inferior colliculus neurons. J Neurophysiol. 1996a; 75:2211–2219. [PubMed: 8793735]

Palombi PS, Caspary DM. Physiology of the young adult Fischer 344 rat inferior colliculus: responses to contralateral monaural stimuli. Hear Res. 1996b; 100:41–58. [PubMed: 8922979]

Paxinos, G.; Watson, C. The rat brain in stereotaxic coordinates. Academic Press; San Diego: 1986.

Pollak GD. The dominant role of inhibition in creating response selectivities for communication calls in the brainstem auditory system. Hear Res. 201310.1016/j.heares.2013.03.001

Pollak GD, Gittelman JX, Li N, Xie R. Inhibitory projections from the ventral nucleus of the lateral lemniscus and superior paraolivary nucleus create directional selectivity of frequency modulations in the inferior colliculus: a comparison of bats with other mammals. Hear Res. 2011; 273:134–144. [PubMed: 20451594]

Portfors CV, Felix RA. Spectral integration in the inferior colliculus of the CBA/CaJ mouse. Neuroscience. 2005; 136:1159–1170. [PubMed: 16216422]

Saldaña E, Aparicio MA, Fuentes-Santamaria V, Berrebi AS. Connections of the superior paraolivary nucleus of the rat: projections to the inferior colliculus. Neuroscience. 2009; 163:372–387. [PubMed: 19539725]

Saldaña E, Berrebi AS. Anisotropic organization of the rat superior paraolivary nucleus. Anat Embryol (Berl). 2000; 202:265–279. [PubMed: 11000278]

Saldaña, E.; Merchan, MA. Intrinsic and commissural connections of the inferior colliculus. In: Winer, JA.; Schreiner, CE., editors. The Inferior Colliculus. Springer; New York: 2005.

Shamma SA, Micheyl C. Behind the scenes of auditory perception. Curr Opin Neurobiol. 2010; 20:361–366. [PubMed: 20456940]

Shannon RV, Zeng FG, Kamath V, Wygonski J, Ekelid M. Speech recognition with primary temporal cues. Science. 1995; 270:303–304. [PubMed: 7569981]

Sivaramkrishnan S, Oliver DL. Distinct K currents result in physiologically distinct cell types in the inferior colliculus of the rat. J Neurosci. 2001; 21:2861–2877. [PubMed: 11306638]

Sun H, Wu SH. Physiological characteristics of postinhibitory rebound depolarization in neurons of the rat's dorsal cortex of the inferior colliculus studies in vitro. Brain Res. 2008; 1226:70–81. [PubMed: 18586018]

Tollin DJ. The lateral superior olive: a functional role in sound source localization. Neuroscientist. 2003; 9:127–143. [PubMed: 12708617]

Walton JP, Frisina RD, Ison JR, O'Neill WE. Neural correlates of behavioral gap detection in the inferior colliculus of the young CBA mouse. J Comp Physiol [A]. 1997; 181:161–176.

Wilson WW, Walton JP. Background noise improves gap detection in tonically inhibited inferior colliculus nerurons. J Neurophysiol. 2002; 87:240–249. [PubMed: 11784746]

Winer, JA.; Schreiner, CE. The central auditory system: a functional analysis. In: Winer, JA.; Schreiner, CE., editors. The Inferior Colliculus. Springer; New York: 2005.

Yang L, Pollak GD. Differential response properties of amplitude modulated signals in the dorsal nucleus of the lateral lemniscus of the mustache bat and the roles of GABAergic inhibition. J Neurophysiol. 1997; 77:324–340. [PubMed: 9120574]

Zhang H, Kelly JB. Glutamatergic and GABAergic regulation of neural responses in inferior colliculus to amplitude-modulated sounds. J Neurophysiol. 2003; 90:477–490. [PubMed: 12660357]

Zhang H, Kelly JB. Responses of neurons in the rat's ventral nucleus of the lateral lemniscus to amplitude-modulated tones. J Neurophysiol. 2006; 96:2905–2914. [PubMed: 16928797]

Zheng Y, Escabi MA. Distinct roles for onset and sustained activity in the neuronal code for temporal periodicity and acoustic envelope shape. J Neurosci. 2008; 28:14230–14244. [PubMed: 19109505]

Zwicker E. Temporal resolution in background noise. Br Audiol. 1985; 19:9–12.

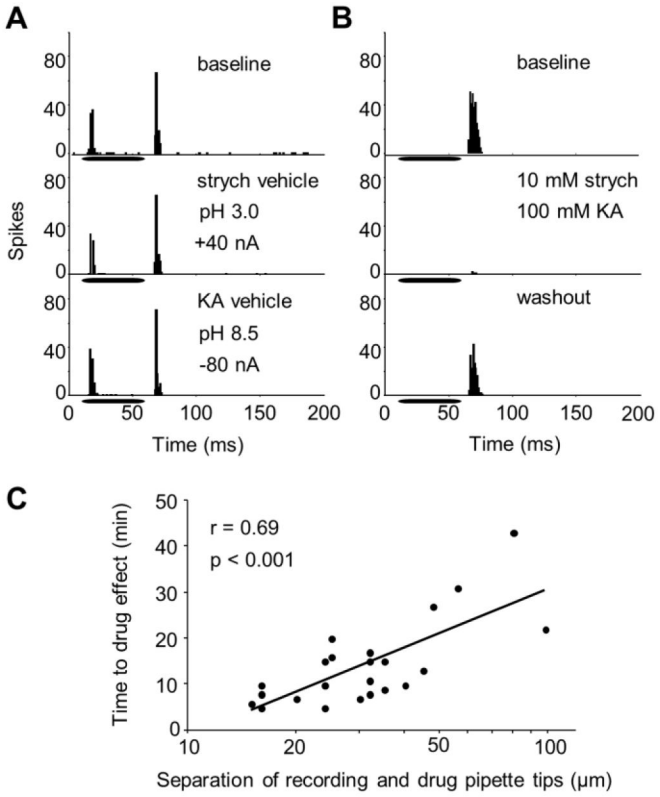

Figure 1. Procedure for pharmacologically inactivating SPON neurons

(A) Compared to the baseline condition (top panel), current-applied vehicle solutions had no effect on SPON spiking (middle and bottom panels; n = 6, Wilcoxon signed-ranks test, $p > 0.9$). (B) Offset spiking prior to drug application (top panel) was abolished following the application of strychnine and kynurenic acid (middle panel). The response magnitude recovered to approach baseline levels following washout of the drugs (bottom panel). (C) The measured distance between the tip of the recording and drug-delivery pipette tips correlated with the amount of time required for drug action (n = 23, Spearman's rank correlation test, $r = 0.69$, $p < 0.01$). Horizontal bars in A, B represent the location of stimuli within the recording windows.

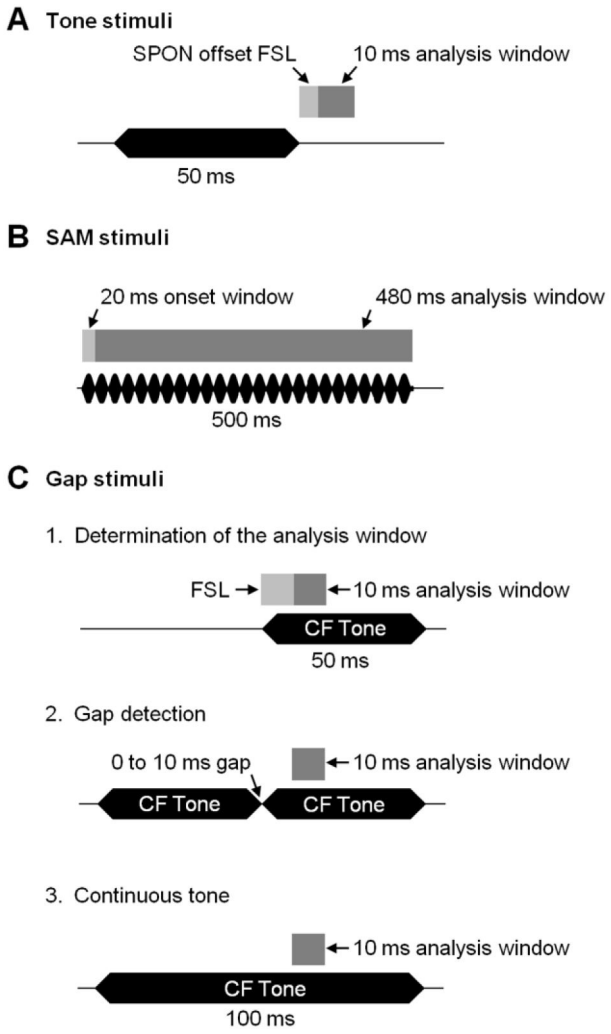

Figure 2. Timing of stimulus presentation and corresponding response analysis windows for inferior colliculus recordings

(A) For pure tone stimuli, a 10 ms analysis window was determined for each IC neuron; it began at the time point corresponding to the shortest first-spike latency (FSL) of the corresponding SPON unit's recorded offset response following the termination of the stimulus. (B) The first 20 ms of responses to SAM signals were excluded from the analysis window to avoid spiking triggered by the onset of the stimulus rather than to individual cycles of amplitude modulation. (C) For gap stimuli, the 10 ms analysis window began when SPON inputs were active in response to the trailing pure tone marker presented in isolation (1, top). This window was kept constant when a second, identical, leading marker was presented along with the trailing marker in the two-tone conditions (2, middle). Spiking to the trailing marker in various gap duration conditions was compared to spiking in a control condition when one continuous tone supplanted the two tones (3, bottom). Dark gray bars represent the analysis windows used in each stimulus condition. Horizontal black bars and rippled bars represent the sound stimuli. CF: characteristic frequency; FSL: first-spike latency.

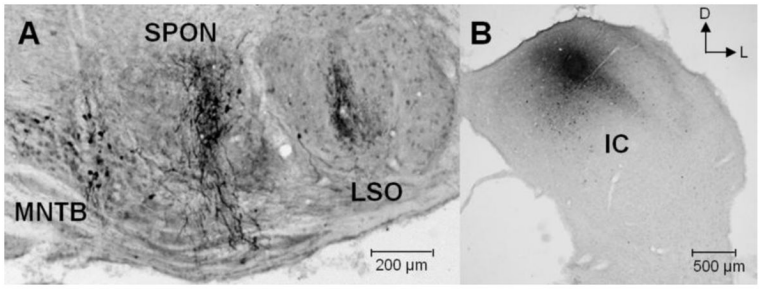

Figure 3. Localization of recording sites in the superior paraolivary nucleus (SPON) and the central nucleus of the inferior colliculus

(A) Typical coronal section through the brainstem at the level of the superior olive shows biocytin deposit sites used to mark the recording locations in the SPON. (B) Corresponding biocytin deposits mark recording locations in the IC. D: dorsal; M: medial; LSO: lateral superior olive; MNTB: medial nucleus of the trapezoid body.

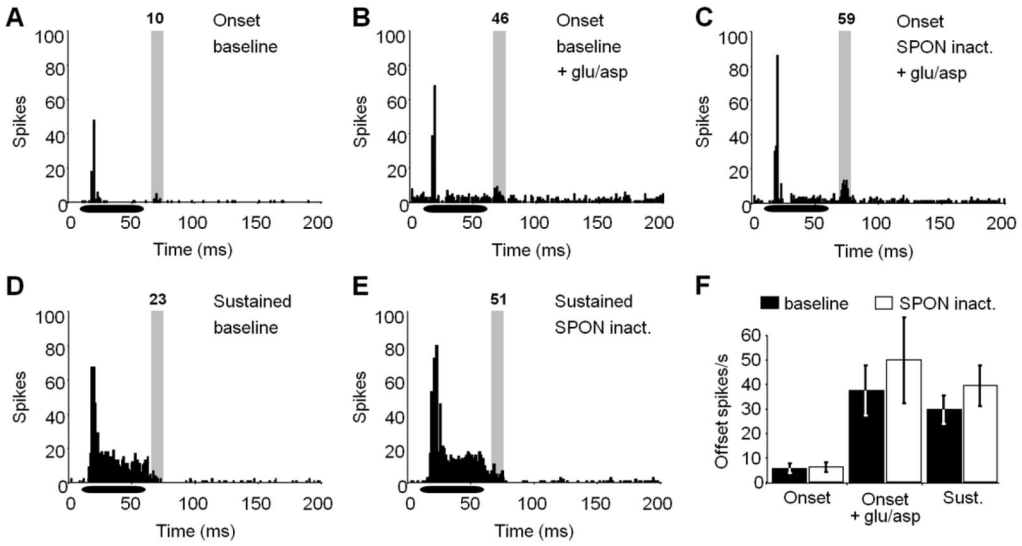

Figure 4. IC neuron responses to pure tones are unaltered during SPON inactivation

(A) A representative onset response to a CF pure tone is shown for the baseline condition. To get a better indication of whether SPON input is manifest following the stimulus offset, overall spiking activity was elevated with iontophoretic application of glutamate and aspartate for baseline (B) and SPON inactivation (C) conditions. A small increase in spiking in the offset analysis window (shaded area) was observed during SPON inactivation. (D) Sustained IC units exhibited high levels of spiking throughout the stimulus presentation and extending into the analysis window. (E) The sustained unit in *D* showed an increase in spiking rate in the analysis window during SPON inactivation. (F) For onset neurons, spiking activity remained low in the offset analysis window before and during SPON inactivation. When glutamate and aspartate were applied by iontophoresis, SPON inactivation caused an increase in spiking, although the change was not significant (Wilcoxon signed-rank test, $p > 0.05$). The average spiking rate was also higher during SPON inactivation for sustained units, but this difference was also not statistically significant. Spike counts are displayed at the top of each analysis window. Horizontal bars represent the location of the stimulus within the recording window. Error bars represent the standard errors of the means.

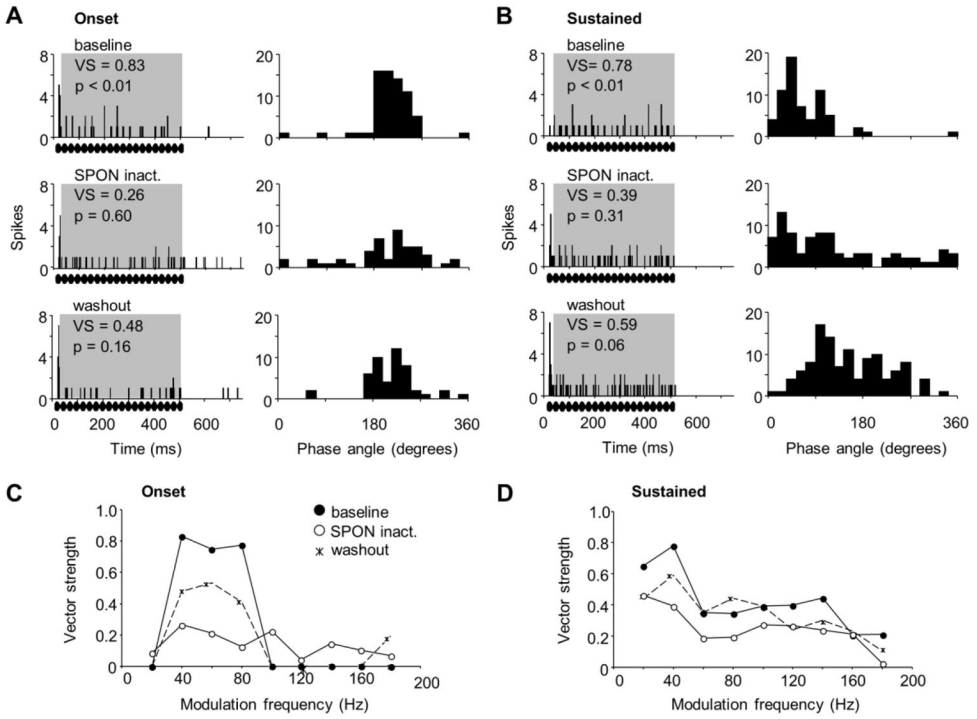

Figure 5. Effects of SPON inactivation on IC unit responses to sinusoidally amplitude modulated (SAM) tones

(A) PSTHs (left) and corresponding phase plots (right) are shown for an onset IC unit's response to a SAM tone of 40 Hz modulation frequency (MF) in the baseline condition (top), during SPON inactivation (middle), and following drug washout (bottom). (B) PSTHs (left) and corresponding phase plots (right) are shown for a sustained IC unit's response to a SAM tone of 40 Hz modulation frequency (MF) in the baseline condition (top), during SPON inactivation (middle), and following drug washout (bottom). (C, D) Vector strengths are shown for the range of MFs presented for baseline, inactivation and recovery conditions for the onset response shown in *A* and the sustained response shown in *B*, respectively. Rippled bars represent the location of the SAM stimulus within the recording window.

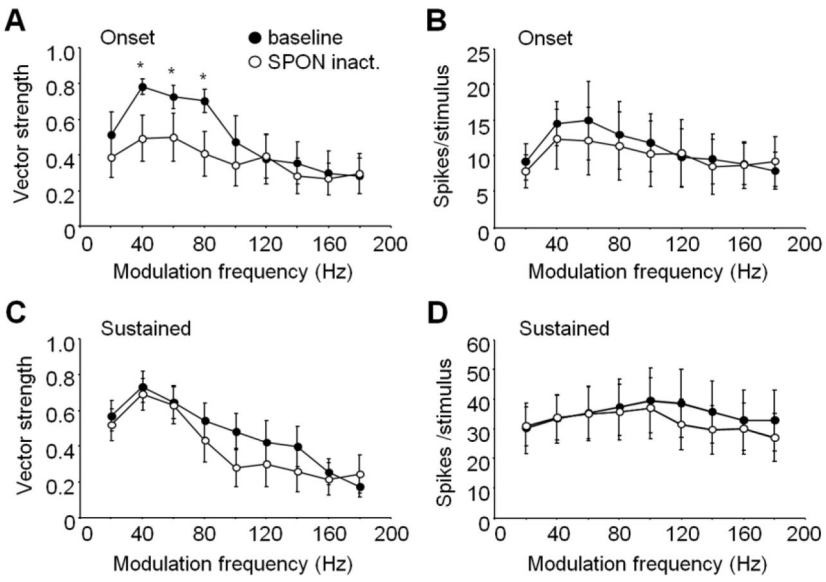

Figure 6. Phase-locking to SAM tones was altered in the IC during SPON inactivation

(A, B) Onset units in the IC displayed reduced vector strengths for low MF SAM tones during SPON inactivation, but spiking activity was unchanged. (C, D) Sustained units showed a trend toward lower vector strengths at higher MFs during inactivation, although the differences did not reach statistical significance (see Results); spiking was also unaffected at any of the MFs presented. All vector strength values greater than 0.6 were phase-locked to the stimulus ($p < 0.05$, Rayleigh test). Asterisks represent significant differences between baseline and SPON inactivation conditions (Wilcoxon signed-rank test, $p < 0.05$). Error bars represent the standard errors of the means.

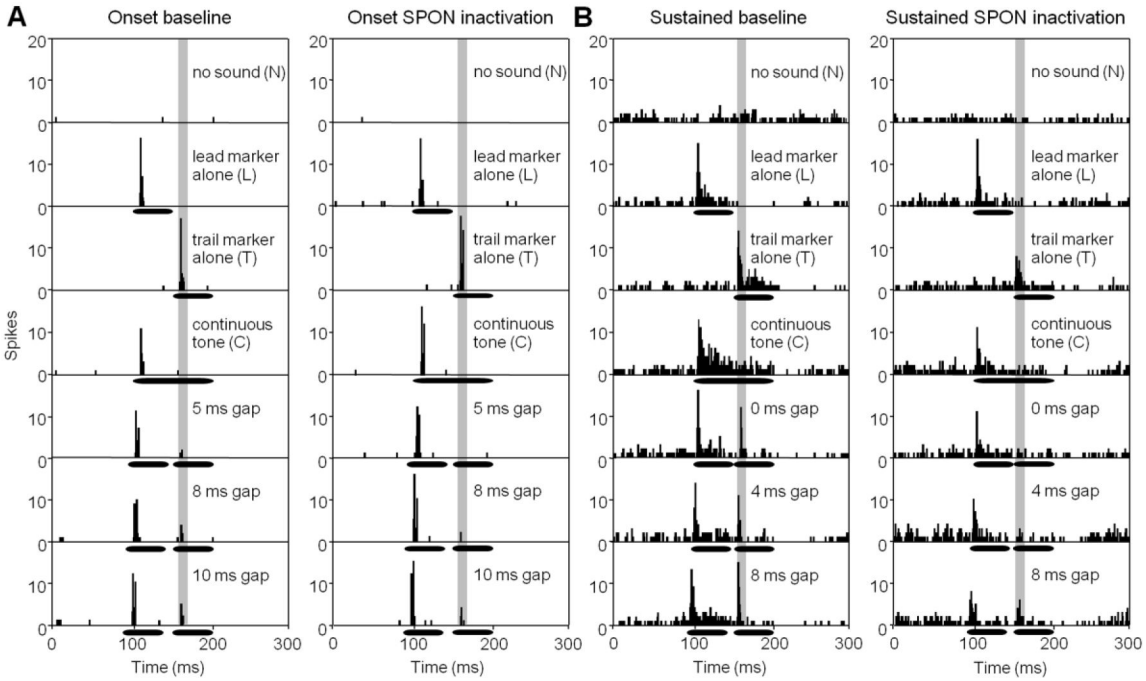

Figure 7. Responses of IC neurons to short gaps in stimuli before and during SPON inactivation

(A) PSTHs are shown for an onset IC unit prior to (left panels) and during SPON inactivation (right panels) for control conditions and for multiple gap durations. (B) Gap test are shown for a sustained IC neuron before (left panels) and during SPON inactivation (right panels). Horizontal bars represent the position of tone stimuli within the recording window.

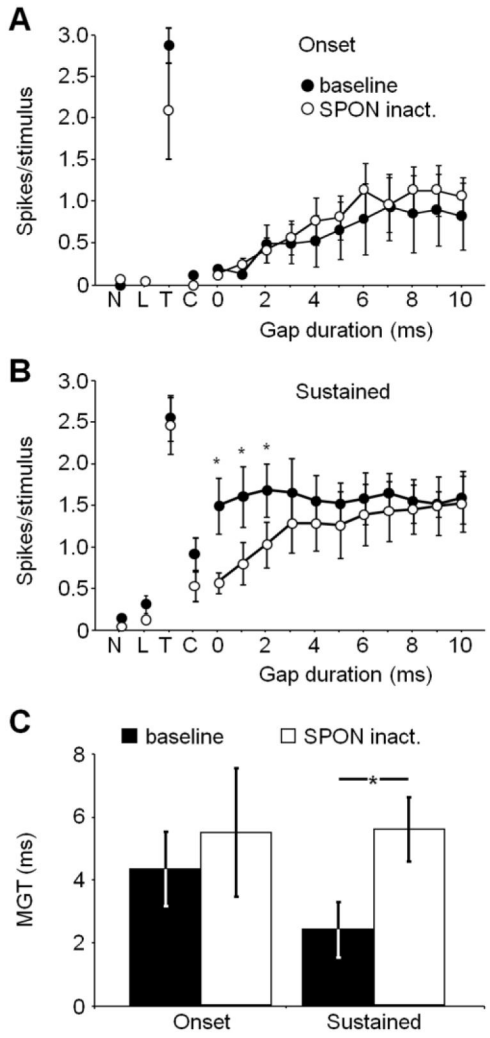

Figure 8.

IC gap detection thresholds were affected by SPON inactivation. (A) Onset neurons exhibited no change in spiking following SPON inactivation for all gap durations. (B) For sustained units, spiking in response to short gap durations (< 4 ms) decreased significantly in the SPON inactivation condition compared to baseline. (C) Mean gap detection thresholds were significantly elevated for sustained, but not onset IC neurons following SPON inactivation (Wilcoxon signed-ranks test, $p < 0.05$). N: no sound; L; leading marker alone; T: trailing marker alone; C: continuous tone; MGT: minimum gap threshold (ms). Error bars represent the standard errors of the means.